Journal of Instrumentation

A large-area planar helicon plasma source with a multi-ring antenna on Linear Experimental Advanced Device (LEAD)

To cite this article: H. Liu *et al* 2020 *JINST* **15** P11002

View the article online for updates and enhancements.

You may also like

- On single-copy entanglement
  Ingo Peschel and Jize Zhao
- A normalization identity for the asymmetric exclusion process on a ring
  T C Dorlas and V B Priezzhev
- A shortcut to the *Q*-operator
  Vladimir V Bazhanov, Tomasz ukowski, Carlo Meneghelli et al.

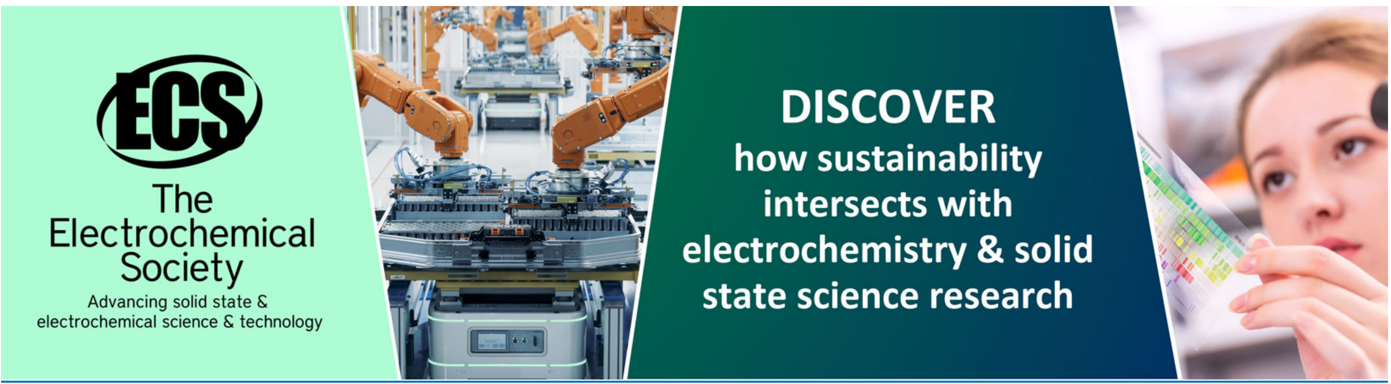

This content was downloaded from IP address 18.117.107.90 on 28/04/2024 at 04:34

Published by IOP Publishing for Sissa Medialab

Received: *July 20, 2020*
Accepted: *August 12, 2020*
Published: *November 2, 2020*

A large-area planar helicon plasma source with a multi-ring antenna on Linear Experimental Advanced Device (LEAD)

2020 JINST 15 P11002

H. Liu,[a,b] **S. Shinohara,**[c] **Y. Yu,**[a,b,1] **M. Xu,**[b,1] **P.F. Zheng,**[b] **Z.H. Wang,**[b] **S.B. Gong,**[b] **H.J. Wang,**[b] **Y.X. Zhu,**[b] **L. Nie,**[b] **R. Ke,**[b] **Y.H. Chen,**[b] **X.R. Duan**[b] **and M.Y. Ye**[a]

[a] *University of Science and Technology of China, Hefei 230026, People's Republic of China*
[b] *Southwestern Institute of Physics, Chengdu 610041, People's Republic of China*
[c] *Tokyo University of Agriculture and Technology, 2-24-16, Naka-cho, Koganei, Tokyo 184-8588, Japan*

E-mail: yuyi@ustc.edu.cn, minxu@swip.ac.cn

Abstract: A planar helicon plasma source with a four-ring antenna has been developed on Linear Experimental Advanced Device (LEAD) in Southwestern Institute of Physics. The diameter of the largest antenna ring is 320 mm. This source is located outside of the vacuum chamber without any vacuum interface and injects radio frequency power into the chamber through a 340-mm-diameter quartz window. A low power threshold of 150 W for electromagnetic-mode to wave-mode transfer is experimentally confirmed. A large volume plasma with a density of over 10^{19} m^{-3} and a plasma generation efficiency (total number of electrons diveded by input power) of over 30×10^{13} W^{-1} indicate the high performance of this large-area helicon plasma source, promising LEAD a suitable device for fundamental plasma physics and plasma material interaction research.

Keywords: Plasma generation (laser-produced, RF, x ray-produced); Plasma diagnostics - probes

[1] Corresponding author.

© 2020 IOP Publishing Ltd and Sissa Medialab
https://doi.org/10.1088/1748-0221/15/11/P11002

Contents

1 Introduction

Radio frequency (RF) plasma sources, which are driven by RF power supplies, can couple RF power to plasma through an antenna and generate plasma by various mechanisms, i.e. electrostatic-mode (E-mode) capacitively coupled plasma, electromagnetic-mode (H-mode) inductively coupled plasma, and wave-mode (W-mode) helicon plasma. Since 1970s, helicon plasma sources are widely used in various fields like fundamental plasma research and industrial plasma processing. In recent years researchers have been working on applying helicon plasma sources to more promising fields like magnetic fusion, space propulsion and space environment simulation. These applications require a helicon plasma source that can produce much larger volume plasma with high efficiency. A conventional helicon plasma source usually generate plasma in a quartz tube with a diameter less than 100 mm. Although there are many kinds of antenna types, the antenna fed by a RF power supply has to be located around the tube, coupling RF energy to the plasma. Building a large-diameter helicon plasma source with this kind of traditional antenna will face various technological difficulties. Large-diameter quartz tube is very difficult to be fabricated, and the coupling efficiency is also questionable since the tube center is far from the antenna surface. Chen had designed a large-area helicon source which consisted of an array of multiple small diameter helicon sources and permanent magnets with a short axial length to produce large-area plasma beam with uniform radial profile for plasma processing, but its reliability under high RF power and high magnetic field might not be satisfactory because of its complexity. Although Watt tried to make a uniform, large-diameter plasma with multiple antennas in the presence of electromagnets, it was successful only with low magnetic field and there is a substantial mutual coupling problem between antennas. Shinohara has developed several large helicon plasma sources with planar spiral antennas, the largest of which had a 430-mm diameter attached to a stainless-steel vessel with a 740 mm inner diameter. He had also developed a segmented multi-loop antenna helicon source with a diameter of 176 mm which could excite selective azimuthal mode number according to experimental requirements.

Planar antennas, including the spiral type and the multi-ring type which will be presented in this article, have various advantages. Firstly, installing a planar antenna at one end of the vacuum

2020 JINST 15 P11002

chamber outside of a quartz window is much easier and cheaper than building a large insulator tube and wrapping the antenna around it, and it is very easy to remove the antenna from the window whenever necessary because there is no vacuum connection between the plasma source and the vacuum chamber. Note that in the case of the large diameter plasma production, it needs much higher power to reach the same electron density, when the antenna is in vacuum and wound around the plasma column, instead of the planar antenna located at the end of the chamber and couple RF energy to the plasma through a quartz window. Secondly, the RF matching circuit can be located just behind an antenna, so that the connecting circuit between matching circuit and antenna can be as short as possible to reduce not only power dissipation but also the difficulty of RF impedance matching. Thirdly, RF power can be deposited in inner radial location compared with antenna which is wrapped around a large insulator tube. Fourthly, by changing the feeding location of the antenna, the radiation field pattern can be adjusted resulting in a controllable plasma radial profile [14, 16]. Fifthly, it is possible to make the aspect ratio (length to diameter ratio) very low which is preferred by plasma thrusters or industrial applications.

In this paper, the development of a large helicon plasma source on Linear Experimental Advanced Device (LEAD), which has a planar multi-ring antenna, is presented. This new helicon source has an antenna system which is more sophisticated and flexible than before, aiming for future high-power operation. The antenna can operate with one to four rings fed (or with other combinations) as well as different current directions (e.g. one is clockwise and another is counter clockwise) to explore the best configuration for high power operation. Considering high voltage in high power operation, the antenna system is designed so that there is a longer creepage distance between antenna rings. Initial results with low RF power of several kW shows its excellent plasma generation efficiency. Large volume plasma with $n_e > 10^{18}\,\mathrm{m}^{-3}$ can be obtained with RF power as low as 150 W, and the density rises to $10^{19}\,\mathrm{m}^{-3}$ when RF power reaches 3000 W. These promising experiments results indicate that with RF power source upgraded to more than 10 kW, the new helicon source can meet the demands of high particle flux (10^{22} to $10^{23}\,\mathrm{m}^{-2}\mathrm{s}^{-1}$) for plasma material interaction (PMI) research.

The rest of this article is arranged as follows. Section 2 is a brief introduction of the LEAD machine. Detailed design of the helicon plasma source is discussed in section 3. Section 4 gives the experimental results of plasma excitation by this source. Section 5 is a brief summary.

2 Experimental setup

The linear plasma device LEAD is a newly built machine for fundamental plasma physics research, diagnostics testing and plasma material interaction (PMI) research. It has a two-stage vacuum chamber as is shown in figure 1. The diameters are 400 mm for the smaller cylindrical chamber stage and 900 mm for the larger chamber stage and the lengths are 2 m and 1 m, respectively. In the experiment presented in this article, argon is used as working gas and it can be fed through both ends of the chamber. 15 magnetic coils which consist of four types can generate different kinds of magnetic configurations [20] and a converging magnetic field configuration is adopted in the experiment presented here, which is favorable for H-W mode transition [21].

A large helicon plasma source, which will be carefully discussed in section 3, is located at the left end of the smaller chamber stage. Between the antenna and the smaller chamber stage, there is

2020 JINST 15 P11002

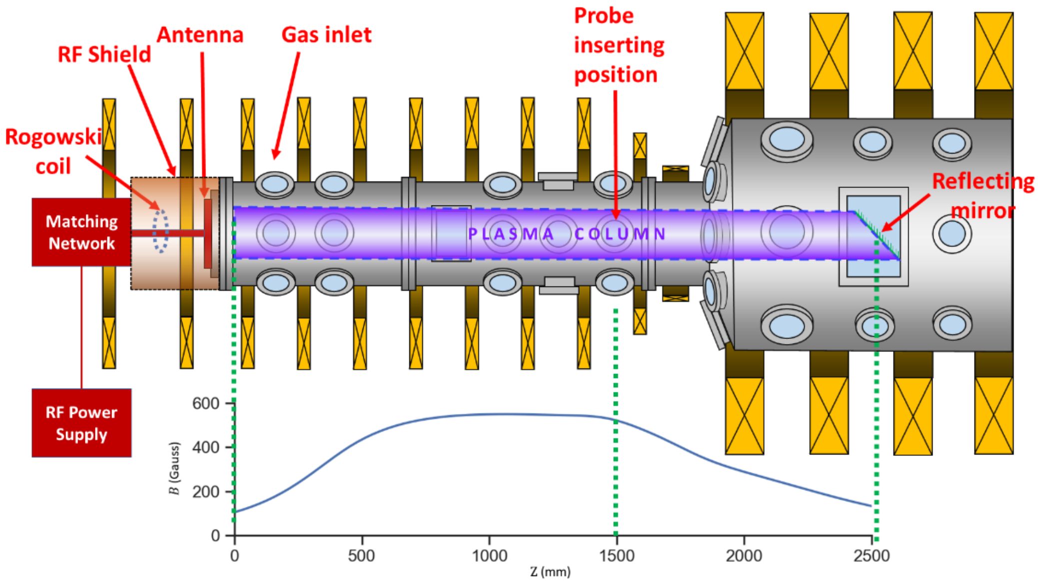

Figure 1. Drawing of the LEAD machine. The magnetic field along the vacuum chamber axis is also shown.

a vacuum-sealing quartz window with a diameter of 340 mm for the RF power to pass through. At the right end of the larger chamber stage, a manipulatable sample plate for PMI research is installed. For this experiment, which is to check the performance of the source, a mirror is fixed on axis of the larger chamber to shade the sample plate from plasma. There is a 45 degrees angle between the mirror surface and the axis, therefore the cross section of the plasma column can be observed by a camera from this mirror through a side window on the larger chamber stage. A scanning single-tip Langmuir probe, which can move radially, is located 1.5 meters away from the source to diagnose main plasma parameters. The probe has a 2 mm-diameter 2 mm-long cylindrical graphite tip. The dimension of this tip is much larger than the Debye length λ_D of dense helicon plasma (typically several µm with density n_e ranging from $10^{18}\mathrm{m}^{-3}$ to $10^{19}\mathrm{m}^{-3}$) and much smaller than gyro radius of ions (larger than 10 mm for a 3 eV ion at a magnetic field of 500 Gs), therefore using Bohm's equation $I_{\mathrm{sat}} = 0.5 n_e e A_p (KT_e/M)^{1/2}$ (n_e, A_p, KT_e and M stands for electron density, probe tip area, electron temperature and ion mass, respectively.) the density can be calculated [22]. The biased voltage scans from −40 V to +40 V at 100 Hz. The probe signal is digitized at 2 MHz and we averaged 100 scans to obtain an I-V curve.

3 Development of the helicon plasma source

A helicon plasma source has been developed to excite and sustain steady-state plasma in LEAD. To meet the experimental requirements of fundamental plasma physics, such as the requirement of a large cross-section plasma for investigation of turbulent physics induced by strong radial density gradient, and the requirement of high particle flux for PMI research, a large-area RF antenna has been designed and fabricated to generate large-volume high-density plasma. This antenna has four concentric copper rings with water-cooling channels inside for long-time steady-state operation. The diameters of the rings are 320 mm, 240 mm, 160 mm and 80 mm, respectively, as is shown in

2020 JINST 15 P11002

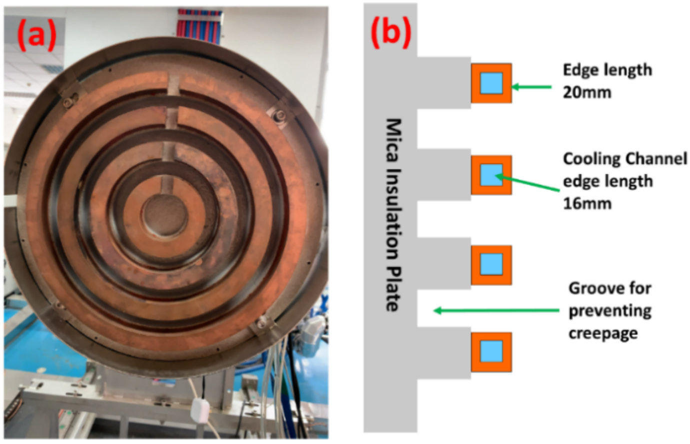

Figure 2. (a) Photo of the four-ring antenna. (b) Drawing of the antenna cross-section.

figure 2(a). Each ring has a square section with an edge length of 20 mm, as is shown in figure 2(b). The inside water channel has an edge length of 16 mm. Cooling water is cycling through the power supply, matching box, antenna and chiller. To feed the antenna, each ring has a cut at 12 o'clock. Feeding points and cooling water connection points are behind these cuts. All rings are fixed on a mica insulation plate. Grooves are designed to increase creepage distance between nearby rings. Different from traditional styles of helicon antennas which always revolve around a quartz tube, this large-area antenna is located at the left end of the smaller chamber stage as shown in figure 1. As has been mentioned in section 2, a flange with a large circular quartz window is used to seal this vacuum end. The diameter and thickness of the quartz window are 340 mm and 16 mm, respectively. The antenna is clung to the window, injecting RF energy into the vacuum to excite plasma.

In the experiment presented in this article, the inner 2 or 3 rings are fed. The RF impedance matching circuit box is located just behind the antenna, and they are connected by copper belt. The split tank automatic matching circuit has a 1300 pF parallel capacitor and a 400 pF serial capacitor, as is shown in figure 3. The matching circuit for 4 rings is under test. The parameters of the full 4-ring plasma will be diagnosed as a future work and will not be discussed in this article.

The assembly of matching box and antenna is installed on rails and can move forward or backward freely, so the assembly can be detached from the window easily for maintenance without breaking vacuum. The 4 rings are electrically connected by copper belt and the connection can be changed freely to excite plasma to meet experimental requirements.

In the initial experiment, the frequency of the RF power supply is 13.56 MHz and the maximal power is 5 kW. It will be upgraded to over 10 kW in the future. Reflected power and forward power measurements are integrated in the RF power supply. Rogowski coils are located between the matching box and antenna to measure antenna current.

4 Experimental results

In this experiment the helicon plasma source is used to excite plasma and there are no ion or electron heating sources, so the ion saturation current is roughly proportional to plasma density according to Langmuir probe theory [1]. Figure 4(a) shows the measured ion saturation current in different

2020 JINST 15 P11002

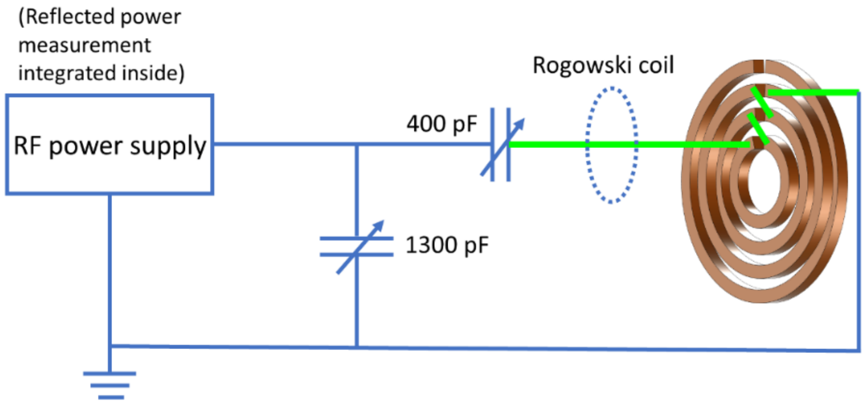

Figure 3. Sketch of matching circuit for the helicon plasma source system. The inner 3 rings are fed in this sketch, and most experiments in this report were performed in this case. The green lines stand for copper belt which can be easily changed to modify antenna configuration.

input RF powers with inner 3 rings fed. The magnetic field is $B_z = 550$G and argon filling pressure is $p_{\mathrm{Ar}} = 1.0$ Pa. The ion saturation current is diagnosed by Langmuir probes at a radial location of $r = 0$. The curve shows a jump at about 150 W indicating the plasma density jump with increasing input power, which is a typical phenomenon in helicon plasma [21]. The mechanism is not very clear yet, but it is a sign of mode change from low-density H-mode inductively coupled plasma (ICP) to high-density W-mode helicon plasma [23]. Noting that conventional helicon sources usually need up to 1000 W to reach this transition [24], this multi-ring large-area helicon source has a one-order lower transition power threshold. After the density jump, the color of plasma light emission observed from side ports changes from blur pink (figure 5(a) and (c)) to bright blue (figure 5(b) and (d)), which is the so-called blue mode and is also observed in many other helicon discharging experiments [24]. The bright blue light mainly comes from argon II emissions, which is related with formation of a radial transport barrier due to interaction of multi-instabilities [25, 26].

With a Rogowski coil between the matching network and the antenna, the RF current can be measured, and the loading resistance can be calculated from the RF current and forward power measurement integrated in the power supply. The antenna vacuum impedance R_{v} measured by a testing circuit consists a function generator, an oscilloscope and a reference resistor is about 2.5 Ohms. The loading resistance can reflect the coupling level between the RF system and the plasma. For the RF power to be deposited in the plasma rather than dissipated in the circuit, the plasma resistance should be at least several Ohms [24]. Figure 4(a) shows the loading resistance with different RF power. Steep increase of loading resistance can be observed in the region below 200 W, which is in coincidence with the density jump shown in figure 4(a). After the density jump, the power efficiency $(R_{\mathrm{Loading}} - R_{\mathrm{v}})/R_{\mathrm{Loading}}$ is over 60%. With RF power over 300 W, the loading resistance goes up to over 10 Ohms and still increase with RF power with a power efficiency higher than 75%, indicating a good coupling level between the antenna and the plasma, considering that in most other helicon experiments the plasma loading resistance is at the level of several Ohms [24].

This helicon plasma source now works as the main plasma source on LEAD. Figure 6 shows measured radial profiles of plasma density with different RF power P_{RF}. As one can see, mean plasma density increases obviously along with the increasing of input power. Density peaking and

2020 JINST 15 P11002

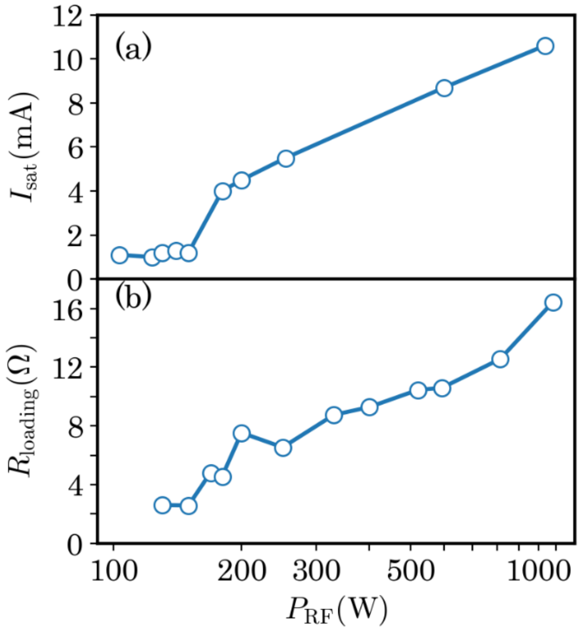

Figure 4. Ion saturation current (a) and loading resistance (b) at different input RF power. Magnetic field B_z = 550 G and argon pressure p_{Ar} = 1 Pa. 3 rings of the antenna are fed.

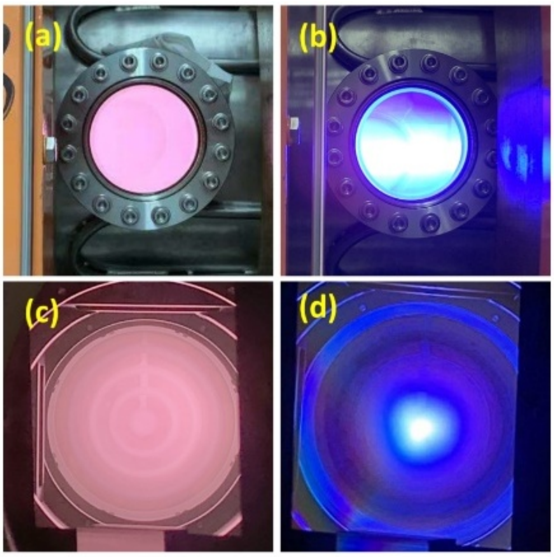

Figure 5. Light emission observed from a side port on the small chamber stage (a, b) and the mirror-side-port system in the larger chamber stage (c, d); pink light before density jump (a, c); bright blue light of helicon plasma (b, d).

2020 JINST 15 P11002

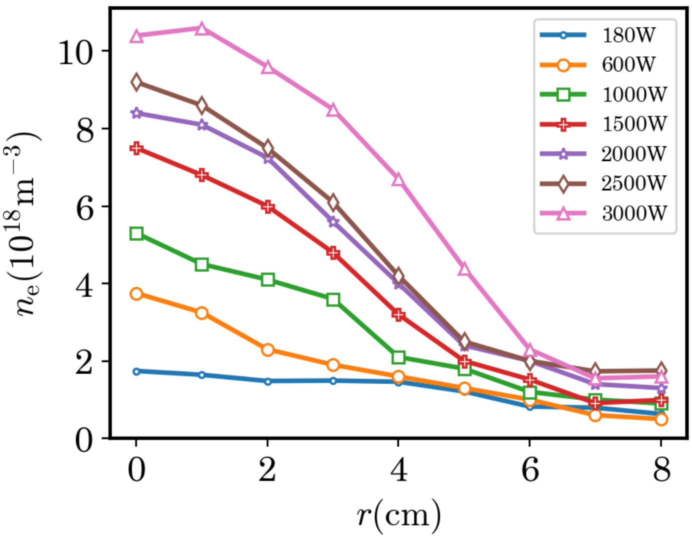

Figure 6. Electron density profiles derived from measured I-V characteristic curves with different input RF powers. Other discharging parameters are B_z = 550 G and p_{Ar} = 1 Pa.

radial gradients appear during helicon discharging, as can be seen from this figure. Note that even the probe is 1.5 m away from the source region, n_e can exceed high density of $10^{19}\,\mathrm{m}^{-3}$. This n_e of $10^{19}\,\mathrm{m}^{-3}$ which is close to boundary plasma density in tokamaks, making this device a suitable platform for plasma turbulence investigation. This is also an acceptable plasma density to form a particle flux of 10^{22} to $10^{23}\,\mathrm{m}^{-2}\mathrm{s}^{-1}$ for PMI research.

Plasma excitation efficiency N_e/P_{inp} is estimated to evaluate this helicon source, where N_e stands for the total number of electrons in the whole plasma column and P_{inp} is the input RF power. Considering that helicon plasma is excited in a vast area and maintains good uniformity along z-axis [14], it can be assumed that the radial profile remains the same along the z-axis from $z = 0$ (antenna location) to $z = 2500$ mm (mirror location). For the 180 W case in figure 7, efficiency of this source is about $30 \times 10^{13}\mathrm{W}^{-1}$, while the efficiency of conventional-type helicon sources with antennas around quartz tubes is less than $10 \times 10^{13}\mathrm{W}^{-1}$ [19]. Shinohara has reported a scaling relationship between N_e/P_{inp} and device section area with data from different devices [19]. This scaling law predicts the upper limit of plasma generation efficiency with given device geometry and can be helpful for designing new devices. We add the data of the LEAD device to this scaling relationship in figure 7 and it agrees well with the scaling. In present experiments, only 3 rings of the antenna are used, and the plasma radius is about 10 cm. In future experiments with full four-ring antenna, we can expect larger plasma radius and the data point will move to right and upper position. The right bottom point deviating from the scaling stands for a helicon plasma source with an antenna in vacuum [18].

Noting that the radius of the smaller chamber stage is 200 mm and the radial integrating range of above estimation is $r < 8$ cm, plasma at outer range ($r > 8$ cm) will also contribute a lot to N_e/P_{RF} and the actual production efficiency is considered to be higher than $30 \times 10^{13}\mathrm{W}^{-1}$.

An advantage of this source is that the connection style of rings can be changed easily. Figure 8 shows the measured radial electron density profiles with inner 2 rings fed (blue solid line and circles) and inner 3 rings fed (red dashed line and diamonds). The input RF power for each case is 2000 W.

2020 JINST 15 P11002

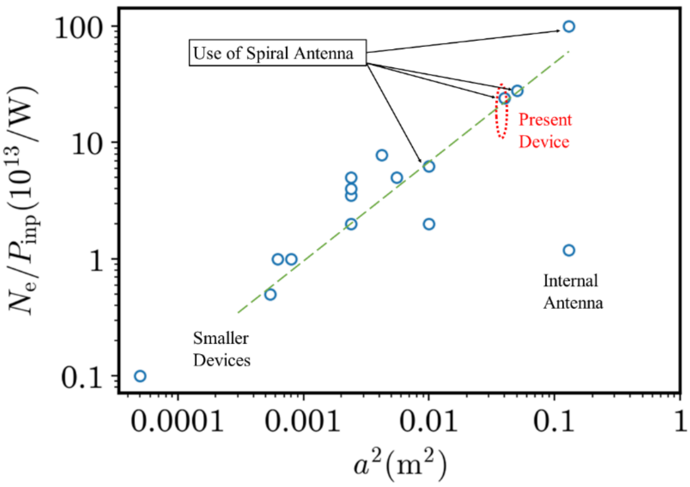

Figure 7. Relationship between plasma generation efficiency N_e/P_{inp} and a^2. N_e, P_{inp} and stands for total number of electrons, input RF power and plasma radius. The green dashed line shows a linear fitting in the power series. The dashed ellipse indicates the data of the present device for which N_e/P_{inp} ranging from 10–30×10^3/W and $a \approx 10\,\text{cm}$.

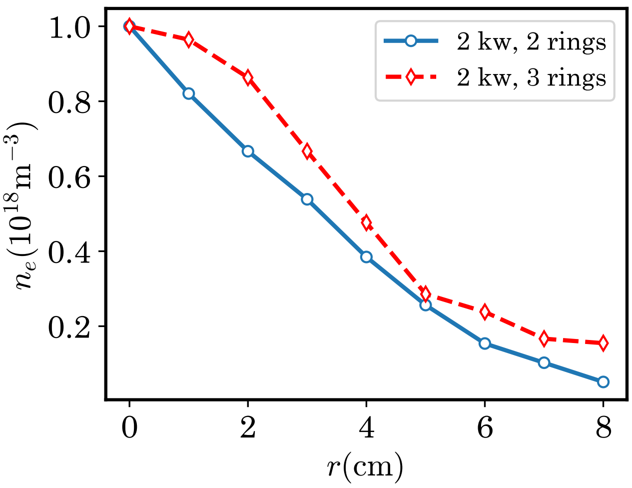

Figure 8. Radial electron density profiles with inner 2 rings fed (blue solid line and circles) and inner 3 rings fed (red dashed line and diamonds).

As one can see, the peak density with 3 rings fed is over 2 times larger than the case with 2 rings fed. In 3-ring case, an obvious density gradient region forms between $r = 2\,\text{cm}$ to $r = 5\,\text{cm}$, implying a possible presence of a plasma shear layer and particle flux transport barrier which could be driven by density gradient induced drift wave turbulence in this region [27]. It is to be noted that the power threshold for density jump is about 1000 W in 2-ring case, while only about 150 W in 3-ring case.

5 Summary and discussion

A large-area helicon plasma source with a multi-ring antenna has been developed on LEAD. In fact, plasma can be effectively excited at an input power of several hundreds of watts by this source.

2020 JINST 15 P11002

When the input power is higher than a threshold, stable W-mode helicon discharge has been achieved. Measurements show that the source can excite a large volume of plasma with a high plasma generation efficiency of $30 \times 10^{13}\,\mathrm{W}^{-1}$.

Although the antenna has 4 rings, only 3 inner rings have been tested in the experiment presented in this article. A 3-ring discharge can produce a much higher plasma density than a 2-ring discharge. The power threshold of transferring from H-mode to W-mode in the 2-ring discharge is about 1000 W, which is similar to some other RF sources reported worldwide. Surprisingly, the 3-ring antenna can effectively reduce the threshold to about 150 W. Although the underlying physics is not clear, a much better plasma production efficiency can be expected for a 4-ring discharge. The characteristics of the 4-ring plasma and the underlying physics are under investigation. The maximal RF power in the initial experiments is 3 kW, though the antenna system is designed to be able to operate at high power over 10 kW. To achieve high power operation, the RF power supply and matching network will be upgraded and the matching network will be adjusted, considering increasing plasma impedance, and higher voltage. Also, an active water-cooling insulator window for high RF energy to pass through is necessary for stable high-power operation. After upgraded, this helicon source could serve as a high particle flux plasma source suitable for fusion-related PMI research.

It is to be noted here that the experiment presented in this article is performed with a certain magnetic field and working gas pressure. Experiments with other external parameters have also been performed. Similar conclusions can be drawn and are not shown here just for simplicity.

Acknowledgments

This work is supported by National Key R&D Program of China under Grant No. 2018YFE0303100, National Natural Science Foundation of China under Grant Nos. 11875124, U1867222, 11705052, 11905051 and 11575055.

References

[1] M.A. Lieberman and A.J. Lichtenberg, *Principles of Plasma Discharges and Materials Processing*, John Wiley & Sons, (2005) [DOI].

[2] H. Bohlin, A. Von Stechow, K. Rahbarnia, O. Grulke and T. Klinger, *VINETA II: A linear magnetic reconnection experiment*, *Rev. Sci. Instrum.* **85** (2014) 023501.

[3] R. Hong, J.C. Li, R.H.C. Thakur, P.H. Diamond and G.R. Tynan, *Generation of parasitic axial flow by drift wave turbulence with broken symmetry: Theory and experiment*, *Phys. Plasmas* **25** (2018) 055710.

[4] S. Inagaki et al., *A Concept of Cross-Ferroic Plasma Turbulence*, *Sci. Rep.* **6** (2016) 22189.

[5] S. Shinohara et al., *High-density helicon plasma sources: basics and application to electrodeless electric propulsion*, *Fusion Sci. Technol.* **63** (2013) 164.

[6] S. Fazelpour, A. Chakhmachi, D. Iraji and H. Sadeghi, *Design and simulation of NBI heating system using high dense helicon plasma source for Damavand Tokamak*, *Fusion Eng. Des.* **137** (2018) 152.

[7] C.G. Jin et al., *Helicon plasma discharge in a toroidal magnetic field of the tokamak*, *IEEE Trans. Plasma Sci.* **39** (2011) 3103.

2020 JINST 15 P11002

[8] F. Díaz et al., *The Development of VASIMR Engine*, in *Proceedings of International Conference on Electromagnetics in Advanced Applications (ICEAA99), Sept. 13–17, 1999, Torino, Italy* **37831**, (1999).

[9] M.D. West, C. Charles and R.W. Boswell, *Testing a helicon double layer thruster immersed in a space-simulation chamber*, *J. Propulsion Power* **24** (2008) 134.

[10] B.D. Blackwell, J.F. Caneses, C.M. Samuell, J. Wach, J. Howard and C. Corr, *Design and characterization of the Magnetized Plasma Interaction Experiment (MAGPIE): a new source for plasma-material interaction studies*, *Plasma Sources Sci. Technol.* **21** (2012) 055033.

[11] F.F. Chen and H. Torreblanca, *Permanent-magnet helicon sources and arrays: a new type of rf plasma*, *Phys. Plasmas* **16** (2009) 057102.

[12] C. Watts, *Alpha: A large-area plasma helicon array*, *Rev. Sci. Instrum.* **75** (2004) 1975.

[13] S. Shinohara and T. Tanikawa, *Development of very large helicon plasma source*, *Rev. Sci. Instrum.* **75** (2004) 1941.

[14] S. Shinohara and T. Tanikawa, *Characteristics of a large volume, helicon plasma source*, *Phys. Plasmas* **12** (2005) 044502.

[15] S. Shinohara, T. Motomura, K. Tanaka, T. Tanikawa and K.P. Shamrai, *Large-area high-density helicon plasma sources*, *Plasma Sources Sci. Technol.* **19** (2010) 034018.

[16] S. Shinohara, T. Tanikawa and T. Motomura, *A segmented multi-loop antenna for selective excitation of azimuthal mode number in a helicon plasma source*, *Rev. Sci. Instrum.* **85** (2014) 093509.

[17] S. Shinohara and T. Soejima, *Trials of RF plasma production using different antenna geometries with magnetic field*, *Plasma Phys. Control. Fusion* **40** (1998) 2081.

[18] B.P. Cluggish et al., *Density profile control in a large diameter, helicon plasma*, *Phys. Plasmas* **12** (2005) 057101.

[19] S. Shinohara et al., *Development of high-density helicon plasma sources and their applications*, *Phys. Plasmas* **16** (2009) 057104.

[20] H. Liu et al., *Design of magnetic configurations for the linear plasma device LEAD*, *Fusion Eng. Des.* **144** (2019) 81.

[21] S. Shinohara, *Helicon high-density plasma sources: physics and applications*, *Adv. Phys. X* **3** (2018) 1420424.

[22] F.F. Chen, *Langmuir probe analysis for high density plasmas*, *Phys. Plasmas* **8** (2001) 3029.

[23] R.L. Kinder, A.R. Ellingboe and M.J. Kushner, *H-to W-mode transitions and properties of a multimode helicon plasma reactor*, *Plasma Sources Sci. Technol.* **12** (2003) 561.

[24] F.F. Chen, *Helicon discharges and sources: a review*, *Plasma Sources Sci. Technol.* **24** (2015) 014001.

[25] S.C. Thakur, C. Brandt, L. Cui, J.J. Gosselin and G.R. Tynan, *Formation of the Blue Core in Argon Helicon Plasma*, *IEEE Trans. Plasma Sci.* **43** (2015) 2754.

[26] S.C. Thakur, C. Brandt, L. Cui, J.J. Gosselin, A.D. Light and G.R. Tynan, *Multi-instability plasma dynamics during the route to fully developed turbulence in a helicon plasma*, *Plasma Sources Sci. Technol.* **23** (2014) 044006.

[27] C. Holland et al., *Observation of Turbulent-Driven Shear Flow in a Cylindrical Laboratory Plasma Device*, *Phys. Rev. Lett.* **96** (2006) 195002.

2020 JINST 15 P11002